

Mechanical and chemical equilibrium in mixtures of active spherical particles: predicting phase behaviour from bulk properties alone

Berend van der Meer,¹ Vasileios Prymidis,¹ Marjolein Dijkstra,¹ and Laura Filion¹

¹*Soft Condensed Matter, Debye Institute for Nanomaterials Science,
Utrecht University, Princetonplein 5, 3584 CC Utrecht, The Netherlands*

We study the phase coexistence of mixtures of active particles using Brownian dynamics simulations. We measure the pressure and the compositions of liquid-gas coexistences and show that they collapse in the pressure-composition plane onto a single binodal in the phase diagram. This confirms that the two phases are in mechanical equilibrium. Additionally, we demonstrate that the coexisting phases are in chemical equilibrium by bringing each phase into contact with particle reservoirs, and showing that for each species these reservoirs are characterized by the same density in both phases. Hence, we show explicitly that the phase separation is governed by bulk properties. Lastly, we show that phase coexistences can be *predicted* quantitatively for torque-free active systems simply by measuring these bulk properties - the same as in equilibrium.

Recent experimental realizations of “active” colloidal particles, i.e. colloidal particles that self-propel, have opened the door to exploiting active building blocks in new colloidal systems (see e.g. [1–4]). These active particles incessantly convert energy into self-propulsion and, as such, systems containing active particles are inherently out-of-equilibrium.

Intriguingly, while active systems often exhibit behaviour fully prohibited in equilibrium systems, such as gas-liquid phase separation in purely repulsive systems (see e.g. [5, 6]) and symmetry-breaking motion [7, 8], the steady-state behaviour of active systems can often be summarized by phase diagrams similar to their passive counterparts, i.e. consisting of single-phase regions and coexistence regions where the lever rule holds. For instance, fairly classic phase diagrams have recently been observed in the attraction-induced liquid-gas phase coexistence of active Lennard-Jones particles [9, 10], the motility-induced phase separation observed in repulsive, self-propelled spheres [5], and even squares [11], as well as binary mixtures [12]. In equilibrium, phase boundaries and coexistences are inherently tied to bulk thermodynamic properties. Since coexisting phases have equal pressures and equal chemical potentials, the bulk properties of the individual phases provide a direct route to predicting phase coexistences - a strategy commonly used to draw phase diagrams. However, for active particles no such rules exist and it remains an open question whether their phase behavior can be predicted from bulk (thermodynamic) quantities. In other words, is it possible to determine whether two phases of active particles coexist purely by measuring their bulk properties?

Perhaps the most studied bulk property in active system is the pressure [13–19]. Recently, Solon and coworkers [13, 15] have shown that there is a well-defined equation of state for torque-free, self-propelled particles. Specifically, for this class of active particles the pressure is purely a function of the bulk density. In this Letter, we take this as a starting point and explore the phase behaviour of an out-of-equilibrium mixture of passive and active attractive particles, and an active-active mixture

of purely repulsive particles. Using computer simulations, we show that, similar to equilibrium, the phase behaviour of these binary mixtures collapses onto a single binodal. Moreover, we demonstrate that the coexisting phases are in chemical equilibrium by bringing each phase into contact with particle reservoirs, and showing that for each species these reservoirs are characterized by the same density in both phases. Hence, we show explicitly that the phase coexistence is governed by bulk properties, which are the pressure and a chemical potential-like bulk variable for each individual species, as represented by the reservoir density. Note that this has been assumed in several approximate theoretical treatments (see e.g. [20–24]). However, to date, no simulations have directly addressed this question, nor verified the existence of a chemical potential-like variable. Furthermore, using the requirement of three sets of equal thermodynamic potentials we *predict* phase coexistences for a torque-free active system simply by measuring bulk properties.

We start this study by looking at three-dimensional systems of N spherical particles that interact via the well-known Lennard-Jones potential:

$$\beta U(r) = 4\beta\epsilon_{LJ} \left(\left(\frac{\sigma}{r} \right)^{12} - \left(\frac{\sigma}{r} \right)^6 \right) \quad (1)$$

truncated and shifted at r_c with σ the particle diameter, $\beta\epsilon_{LJ}$ the energy scale, and $\beta = 1/k_B T$, where k_B is the Boltzmann constant and T is the temperature. Out of the N particles, we “activate” a subset of N_a particles by introducing a constant self-propulsion force f_a along the self-propulsion axis $\hat{\mathbf{u}}_i$. We denote the fraction of active particles by $x = N_a/N$. The system is simulated using overdamped Brownian dynamics. Specifically, the equations of motion for particle i are:

$$\dot{\mathbf{r}}_i(t) = \beta D_0 [-\nabla_i U(t) + f_i \hat{\mathbf{u}}_i(t)] + \sqrt{2D_0} \boldsymbol{\xi}_i(t) \quad (2)$$

$$\dot{\hat{\mathbf{u}}}_i(t) = \sqrt{2D_r} \hat{\mathbf{u}}_i(t) \times \boldsymbol{\eta}_i(t), \quad (3)$$

where $\boldsymbol{\xi}_i(t)$ and $\boldsymbol{\eta}_i(t)$ are stochastic noise terms with zero mean and unit variance. Note that for passive particles $f_i = 0$, and for active particles $f_i = f_a$. The translational diffusion coefficient D_0 and the rotational diffusion

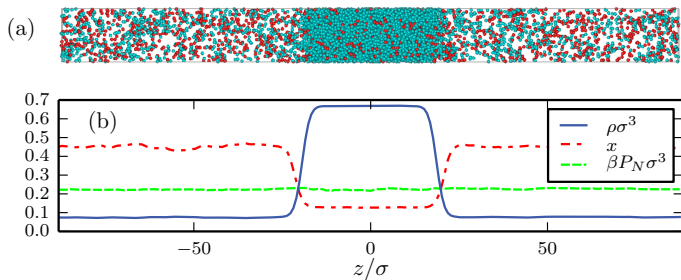


FIG. 1: (a) Liquid-gas coexistence of an active-passive mixture with an overall active fraction $x = 0.22$ at an overall density $\rho\sigma^3 = 0.20$. For the active particles the self-propulsion force equals $f_a = 10k_B T/\sigma$. (b) The corresponding density, composition, and pressure profile along the long direction z of the box. The system contains $N = 8192$ particles.

constant D_r are linked via the Stokes-Einstein relation $D_r = 3D_0/\sigma^2$. We measure time in units of the short-time diffusion $\tau = \sigma^2/D_0$. Note that we define the total density of the system $\rho = N/V$, where V is the volume of the system. Moreover, we define the partial active and passive densities $\rho_a = x\rho$ and $\rho_p = (1-x)\rho$, respectively.

To start our investigation we construct a liquid-gas coexistence in an active-passive mixture, in the regime where the system phase separates due to attractions [9]. To this end, we set the interaction cutoff radius $r_c = 2.5\sigma$ and the energy scale $\beta\epsilon_{LJ} = 1.2$, which for a purely passive system ($x = 0$) results in a well-characterized liquid-gas coexistence at intermediate densities [25]. In the following we fix the self-propulsion force $f_a = 10k_B T/\sigma$ for all active particles, and perform simulations for a range of values of the active fraction x and overall system density ρ in an elongated simulation box. For more simulation details we refer to the Supplementary Materials (SM) [26].

In Figure 1(a), we show a typical snapshot of an active-passive mixture exhibiting a liquid-gas coexistence. Here, the active and passive particles are plotted as red and blue, respectively. In Figure 1(b), we plot the corresponding density $\rho(z)$, active particle fraction $x(z)$, and the normal pressure $P_N(z)$ along the long axis of the box. The expression and derivation of the normal pressure can be found in the SM [26], where we have used methods presented in Refs. 27–29. Note that in the bulk regime of either phase, this normal pressure P_N will be equal to the bulk pressure P of the phase in question. Figure 1(b) shows that, in this case, the system exhibits a gas-liquid coexistence with the gas characterized by density ρ^G and composition x^G , and the liquid characterized by density ρ^L and composition x^L . We always find the gas phase to be more rich in active particles, which is reminiscent of segregation phenomena seen in other studies of active mixtures [30, 31]. Note that in all of our simulations, the pressure is the same in both coexisting phases indicating that the system is in mechanical equilibrium.

Using composition and pressure profiles, similar to those shown in Figure 1(b), we map out the coexist-

ing compositions and pressures of our active-passive mixtures, for a wide range of overall system densities ρ and compositions x . The results are plotted in Figure 2(a). Similar to passive systems, we find that the phase behaviour collapses in this representation, i.e. the lever rule holds within the coexistence region.

The validity of the lever rule is also evident when plotting the phase diagram in the active density - passive density ($\rho_a - \rho_p$) representation, as shown Figure 2(b). This is consistent with the recent simulation results of Ref. 12 where they summarized the phase behaviour of a different active-passive mixture in the $\rho_a - \rho_p$ representation. We also investigate the pressure dependence of the partial densities of each species in the coexisting liquid and gas phases. In Figure 2(c) we plot these partial densities ρ_i^γ vs. pressure P with i denoting the species (active or passive) and γ denoting the phase (liquid(L) or gas(G)). Interestingly, we find that in the gas phase, the partial densities of the active and passive species are approximately the same along the entire coexistence curve.

Our results so far clearly demonstrate that the pressure is a key variable in controlling phase coexistences in our active-passive mixture: all phase coexistences are characterized by equal bulk pressures in the two phases. However, phase coexistence in an equilibrium binary system requires not only equal pressures between the two phases, but also equal chemical potentials for both species. This raises the question whether we can identify bulk properties analogous to the chemical potential in active-passive mixtures which similarly control the phase coexistence.

The standard method for showing chemical equilibrium in passive systems is to measure the chemical potential in both phases, for both species. For a passive system, this can be done in a number of different ways depending on the exact circumstance - ranging from e.g. grand canonical simulations to thermodynamic integration [32]. However, for active systems the situation is much more complex and currently there is no well-established method to measure the chemical potential. To avoid this issue, we go back to more basic definitions of the chemical potential. In a textbook derivation of the chemical potential, one typically attaches the system in question to a large particle reservoir, and allows the particles of a given species to travel between the subsystem in question, and the particle reservoir. The subsystem is then in a grand-canonical (μVT) ensemble, with μ set by the chemical potential of the reservoir. Hence, if two systems have the same chemical potential, one must be able to connect them to the same particle reservoir, i.e. one with the same particle density. Here, we follow a similar procedure with our simulations. Specifically, we select a binary gas and liquid that coexist, and connect them to particle reservoirs that only contain a single species. Note that in total we will need four simulations per coexistence point, namely: the gas in contact with a passive particle reservoir, the gas in contact with an active particle reservoir, the liquid in contact with a passive particle reservoir, and the liquid in contact with an active par-

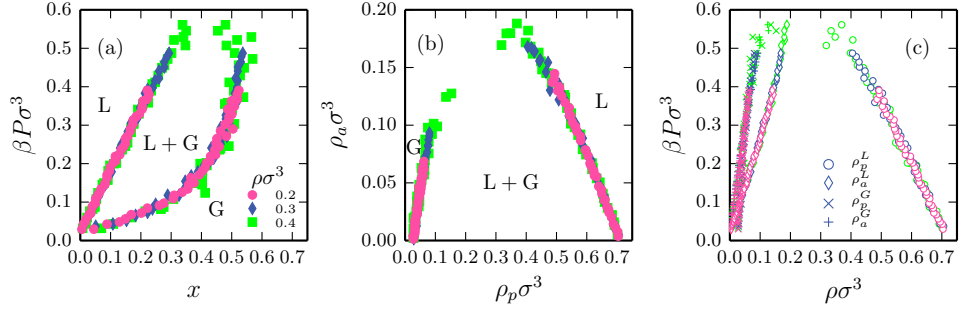


FIG. 2: (a) Phase diagram of the Lennard-Jones active-passive mixture in the P - x representation. (b) The same phase diagram in the ρ_a - ρ_p representation. (c) Coexistence lines in the P - ρ_a and P - ρ_p representations.

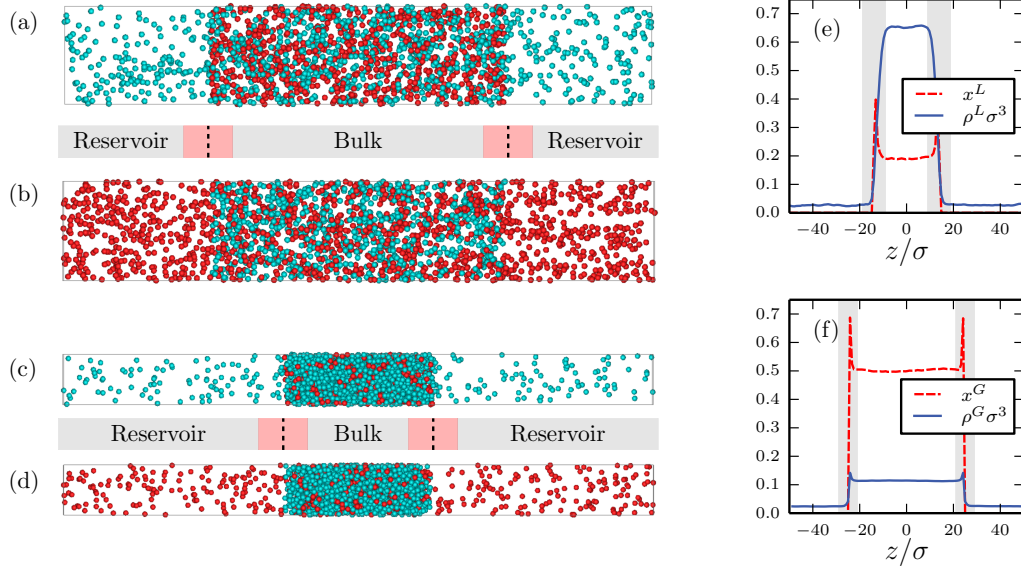


FIG. 3: (a) The gas in contact with a passive particle reservoir. (b) The gas in contact with an active particle reservoir. (c) The liquid in contact with a passive particle reservoir. (d) The liquid in contact with an active particle reservoir. Note that the reservoirs associated with the gas (a,b) and liquid (c,d) phase have different cross-sections, making the reservoir densities in (a,b) seem a lot higher compared to those in (c,d) – even though they are equal. (e,f) Density and composition profiles of the liquid (e) and gas (f) in contact with a passive reservoir. The partial densities of the binary phases were chosen to correspond to the coexistence at pressure $\beta P \sigma^3 = 0.34$. Note that some active particles adsorb at the wall. We thus exclude these interfacial regions (shaded areas) in the determination of the bulk density and composition, as well as in the determination of the reservoir density.

ticle reservoir. The goal will be to determine whether the active (and passive) reservoirs associated with the coexisting phases are the same. If they are, then we can infer that there exists a chemical potential-like variable that governs the coexistence. Note that this method relies on the system being multicomponent, as for a single-component system, the reservoir and the system in this method would be by definition identical.

To this end, we divide our simulation box into two sections, one which contains the “bulk” liquid or gas phase, with the other part of the box acting as a passive (or active) particle reservoir (see Figure 3(a-d)). We place a semi-permeable membrane at the division which only allows one of the two species, which we call species R , to pass through at no energy cost. For the other species,

the wall is impenetrable with the wall-particle interaction given by the purely repulsive Weeks-Chandler-Andersen-like wall potential:

$$\beta U(z) = 4\beta\epsilon_{WCA} \left(\left(\frac{\sigma}{z} \right)^{12} - \left(\frac{\sigma}{z} \right)^6 + \frac{1}{4} \right), \quad (4)$$

where z is the distance of a particle in the bulk to the nearest semi-permeable wall, $\beta\epsilon_{WCA} = 40$, and the interaction is cut off at a distance $z = 2^{1/6}\sigma$. During the simulation we measure the partial densities of each species in the center of the bulk phases (i.e. away from the semi-permeable membrane). We then tune the density of the reservoir so that the partial density of species R in the bulk matches the targeted partial density. During equilibration, a small fraction of the bulk phase builds up on

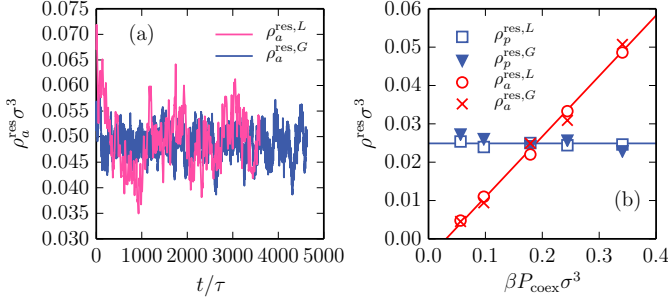


FIG. 4: (a) The density in the active particle reservoir over time for both the liquid and the gas. Both phases converge to the same reservoir density of active particles. (b) The reservoir densities as a function of the coexistence pressure P_{coex} . The liquid and gas phase are in contact with the same reservoirs, showing that there is chemical equilibrium between the phases, for each species. Please note that while the passive particle reservoir density is essentially constant, the active particle reservoir density increases rapidly with increasing coexistence pressure. This hints that for this system the bulk properties of the system are essentially dictated by the active particles.

the semi-permeable membrane, and sometimes depletes the bulk region of the confined species. To counteract this adsorption (depicted in Figure 3 (e,f)) and ensure that the bulk phase has the correct density and composition far away from the semi-permeable membrane, we also tune the number of particles of the confined species during equilibration. Eventually, the average partial densities of both species in the bulk region reach a constant.

In Figure 4(a), we show the time evolution of the densities in the active particle reservoirs for the coexisting liquid and gas phases at $\beta P \sigma^3 = 0.34$. Note that although we chose a high initial density of the reservoirs in both cases, both reservoir densities quickly converged to the same density. In Figure 4(b), we plot the densities of both the active and passive reservoirs as a function of the coexistence pressure P_{coex} . Clearly, for all coexisting liquid-gas pairs we find the same reservoir densities: $\rho_p^{\text{res},L} = \rho_p^{\text{res},G}$ and $\rho_a^{\text{res},L} = \rho_a^{\text{res},G}$. Hence, while we still cannot directly measure the chemical potential of our active systems, this demonstrates the existence of a bulk variable that is conjugate to the number of particles in these active systems, thereby providing clear simulation evidence of an active chemical potential.

So far, we have shown that gas-liquid coexistence for an active-passive mixture of Lennard-Jones particles is entirely controlled by properties which can be measured purely in the individual coexisting phases, namely the bulk pressure and reservoir densities per species. This of course raises the interesting question whether or not such phase coexistence rules can also be found for systems undergoing a motility-induced phase separation, and whether or not they can be used to predict the phase diagram.

To this end, we use the Weeks-Chandler-Andersen po-

tential with the interaction cutoff radius $r_c = 2^{1/6} \sigma$ and the energy scale $\beta \epsilon_{\text{WCA}} = 40$. Here, we consider a two dimensional active-active mixture with the self-propulsions of fast and slow species being $f_f = 160 k_B T / \sigma$ and $f_s = 120 k_B T / \sigma$, respectively. Note that in this case we find a phase separation between a high density crystal phase and a low density gas phase. For more simulation details we refer to the SM [26]. For this active-active mixture, we observe a clear collapse of the direct coexistence data onto a single binodal, as summarized in the phase diagram in Figure 5(a).

As a next step we predict the phase boundaries by calculating the pressure P and reservoir densities ρ_f^{res} and ρ_s^{res} for a wide range of binary crystal and gas phases (shaded area in Figure 5(a)). We summarize the results in Figure 5(b), where the red and blue surfaces correspond to the gas and crystal phase, respectively. The intersection between the two surfaces implies a phase coexistence between the two phases. Namely, for these points mechanical and chemical equilibrium are satisfied: both the pressure as well as the two reservoir densities are equal.

The resulting binodals are in good agreement with the direct coexistence data [Figure 5(a)]. We thus have predicted the phase diagram for an active-active mixture undergoing motility-induced phase separation. This result highlights that also for these systems, which are extremely far from equilibrium, simple coexistence rules are satisfied. Therefore, this result sheds new light on the thermodynamics of systems of active spherical particles.

In conclusion, we have demonstrated, for the first time, that the phase coexistence of active spherical particles is fully governed by mechanical and chemical equilibrium. Specifically, our results clearly show that phase coexistence for mixtures of active particles is entirely controlled by properties which can be measured purely in the individual coexisting phases, namely the bulk pressure and

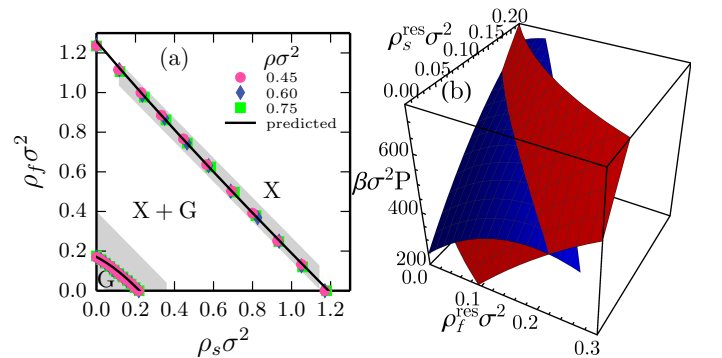


FIG. 5: (a) Direct coexistence results for the phase diagram of the active-active mixture of WCA particles (markers), and the predicted phase diagram (line). Note that X denotes the crystal phase while G denotes the gas phase. (b) Surface plots of the gas (red) and crystal (blue) reservoir densities vs pressure. From the intersection between the two surfaces we obtain the predicted binodals in (a).

reservoir densities per species. Using this requirement of three sets of equal thermodynamic potentials we have quantitatively *predicted* phase coexistences for torque-free active systems simply by measuring bulk properties - the same as in equilibrium.

Acknowledgements: We acknowledge funding from the Dutch Sector Plan Physics and Chemistry, and L.F. acknowledges financial support from the Netherlands Organization for Scientific Research (NWO-VENI Grant No. 680.47.432). We would like to thank Frank Smallen-

burg for many useful discussions and carefully reading the manuscript.

Author Contributions: BvdM and VP contributed equally to this work. LF designed and supervised the project. MD devised the simulations of the particle reservoirs to demonstrate that the coexisting phases are in chemical equilibrium with the same particle reservoirs. BvdM and VP carried out the simulations and did the analysis. All authors co-wrote the paper.

-
- [1] M. C. Marchetti, J. Joanny, S. Ramaswamy, T. Liverpool, J. Prost, M. Rao, and R. A. Simha, *Rev. Mod. Phys.* **85**, 1143 (2013).
 - [2] I. S. Aranson, *Phys. Usp.* **56**, 79 (2013).
 - [3] J. Elgeti, R. G. Winkler, and G. Gompper, *Rep. Prog. Phys.* **78**, 056601 (2015).
 - [4] J. Bialké, T. Speck, and H. Löwen, *J. Non-Cryst. Solids* **407**, 367 (2015).
 - [5] G. S. Redner, M. F. Hagan, and A. Baskaran, *Phys. Rev. Lett.* **110**, 055701 (2013).
 - [6] M. E. Cates and J. Tailleur, *Annu. Rev. Condens. Matter Phys.* **6**, 219 (2015).
 - [7] C. Reichhardt and C. O. Reichhardt, *Phys. Rev. E* **88**, 062310 (2013).
 - [8] R. Di Leonardo, L. Angelani, D. DellArciprete, G. Ruocco, V. Iebba, S. Schippa, M. Conte, F. Mecarini, F. De Angelis, and E. Di Fabrizio, *Proc. Natl. Acad. Sci. U.S.A.* **107**, 9541 (2010).
 - [9] V. Prymidis, H. Sielcken, and L. Filion, *Soft Matter* **11**, 4158 (2015).
 - [10] V. Prymidis, S. Paliwal, M. Dijkstra, and L. Filion, *J. Chem. Phys.* **145**, 124904 (2016).
 - [11] V. Prymidis, S. Samin, and L. Filion, *Soft Matter* **12**, 4309 (2016).
 - [12] B. Trefz, S. K. Das, S. A. Egorov, P. Virnau, and K. Binder, *J. Chem. Phys.* **144**, 144902 (2016).
 - [13] A. P. Solon, J. Stenhammar, R. Wittkowski, M. Kardar, Y. Kafri, M. E. Cates, and J. Tailleur, *Phys. Rev. Lett.* **114**, 198301 (2015).
 - [14] S. C. Takatori, W. Yan, and J. F. Brady, *Phys. Rev. Lett.* **113**, 028103 (2014).
 - [15] A. P. Solon, Y. Fily, A. Baskaran, M. E. Cates, Y. Kafri, M. Kardar, and J. Tailleur, *Nat. Phys.* **11**, 673 (2015).
 - [16] J. Bialké, J. T. Siebert, H. Löwen, and T. Speck, *Phys. Rev. Lett.* **115**, 098301 (2015).
 - [17] G. Falasco, F. Baldovin, K. Kroy, and M. Baiesi, *arXiv:1512.01687*.
 - [18] T. Speck and R. L. Jack, *Phys. Rev. E* **93**, 062605 (2016).
 - [19] R. G. Winkler, A. Wysocki, and G. Gompper, *Soft Matter* **11**, 6680 (2015).
 - [20] J. Tailleur and M. Cates, *Phys. Rev. Lett.* **100**, 218103 (2008).
 - [21] J. Stenhammar, A. Tiribocchi, R. J. Allen, D. Marenduzzo, and M. E. Cates, *Phys. Rev. Lett.* **111**, 145702 (2013).
 - [22] R. Wittkowski, A. Tiribocchi, J. Stenhammar, R. J. Allen, D. Marenduzzo, and M. E. Cates, *Nat. Commun.* **5**, 4351 (2014).
 - [23] U. M. B. Marconi and C. Maggi, *Soft Matter* **11**, 8768 (2015).
 - [24] S. C. Takatori and J. F. Brady, *Soft Matter* **11**, 7920 (2015).
 - [25] B. Smit, *J. Chem. Phys.* **96**, 8639 (1992).
 - [26] Supplementary Materials (link here).
 - [27] D. S. Dean, *J. Phys. A: Math. Gen.* **29**, L613 (1996).
 - [28] A. M. Menzel, *Phys. Rev. E* **85**, 021912 (2012).
 - [29] T. Ikeshoji, B. Hafskjold, and H. Furuho, *Molecular Simulation* **29**, 101 (2003).
 - [30] S. R. McCandlish, A. Baskaran, and M. F. Hagan, *Soft Matter* **8**, 2527 (2012).
 - [31] J. Stenhammar, R. Wittkowski, D. Marenduzzo, and M. E. Cates, *Phys. Rev. Lett.* **114**, 018301 (2015).
 - [32] D. Frenkel and B. Smit, *Understanding Molecular Simulations: From Algorithms to Applications* (Academic Press, San Diego, 2002).